Available online at www.sciencedirect.com
ScienceDirect
Ceramics International 35 (2009) 2943–2950
CERAMICS INTERNATIONAL
www.elsevier.com/locate/ceramint

Neural network modeling and analysis of gel casting preparation of porous Si_3N_4 ceramics

Juanli Yu [a], Hongjie Wang [a,*], Jian Zhang [b]

[a] State Key Laboratory for Mechanical Behavior of Materials, School of Materials Science and Engineering, Xi'an Jiaotong University, 28 Xian Ning Road, Xi'an 710049, China
[b] National Key Laboratory of Advanced Functional Composite Materials, Beijing 100076, China

Received 30 January 2009; received in revised form 3 March 2009; accepted 2 April 2009
Available online 24 April 2009

Abstract

Based on orthogonal experimental results of porous Si_3N_4 ceramics by gel casting preparation, a three-layer back propagation artificial neural network (BP ANN) was developed for predicting the performances of porous Si_3N_4 ceramics. The results indicated that BP ANN was a very useful and accurate tool for the prediction and optimization of porous Si_3N_4 ceramics performances. By using the developed ANN model, the influences of the compositions on performances of porous Si_3N_4 ceramics were investigated, and some important conclusions were drawn as follows: for the flexural strength of Si_3N_4 ceramics, solid loading has an optimum value where can achieve a maximum value, and the optimum solid loading decreases with the increase of monomer content; the porosity of sintering body monotonically decreases with the increase of solid loading, and it increases with monomer content; the porosity of sintering body monotonically increases with the increase of the ratio of crosslinking agent to monomer.

Keywords: B. Porosity; C. Strength; Artificial neural networks; Gel casting; Si_3N_4 ceramics

1. Introduction

Silicon nitride (Si_3N_4) ceramics have excellent mechanical properties (such as high strength, high fracture toughness, high thermal shock resistance, and high chemical resistance), and then they have great promise for engineering applications [1,2]. Porous Si_3N_4 ceramics with certain levels of porosity offer an interesting combination of strength and stiffness, and they are lighter and also can be machined more easily than dense Si_3N_4 ceramics [3].

So far, a number of routes for the porous ceramics such as foaming, stacking of presintered granules or fibers, aerogel or sol–gel and pyrolysis of various organic additives, and gel casting have been developed [1–5]. Among these preparation approaches, the gel casting is an innovative approach to the preparation of porous ceramics [6]. During gel casting based on the in situ polymerization of organic monomer binder, the monomers are polymerized to form a rather strong cross-linked polymer network that permanently immobilizes the ceramic particles in the shape defined by the mold [7]. Therefore, gel casting shows the ability to fabricate homogeneous and complex-shaped green body with high green strength [8].

The process of gel casting technique consists of the dispersion of ceramic powder in an aqueous monomer solution to form a fluid and castable slurry that is subsequently gelled in the mold. A homogeneous wet cast body is formed, and the wet cast body has homogeneous chemistry and density that contains a certain percent of organic binder. After drying, binder removal and sintering take place as in other ceramic processes. Pores in ceramic are formed during drying and organic binder removal from green body. Recently, gel casting technique has been extensively used in producing porous ceramic parts of drug delivery systems, bio-ceramics and sensors, ceramic foams, and porous support and filter systems for membranes [9–12].

So far, during the preparation of porous ceramics by gel casting, a number of routes for the porous ceramics (such as foaming, stacking of presintered granules or fibers, aerogel or

* Corresponding author. Tel.: +86 29 82667942; fax: +86 29 82665443.
E-mail address: yujuanlli@126.com (H. Wang).

0272-8842/$36.00.
doi:10.1016/j.ceramint.2009.04.008

sol–gel and pyrolysis of various organic additives) have been developed [4,5]. However, little work was focused on the investigation of the porous ceramics preparation by merely increasing monomer content in the slurry without other organic additives during gel casting. Here, monomer and crosslinking agent not only can form macromolecular network to hold the ceramic particles together, but also can play the leading role in the formation of pores during the fabrication of porous Si_3N_4 ceramics. The preparation approach can make the pore size distribution more uniform. Investigation of the preparation approach is currently attracting a great deal of attention. In order to improve the performance of porous Si_3N_4 ceramics, it is important to predict accurately flexural strength and porosity using analytical or numerical tools that take into account the complexity of compositions.

Artificial neural networks (ANNs) are extensively used in solving diverse areas of science and engineering problem [13,14]. In the paper, in order to investigate the porous ceramics preparation by increasing monomer content in the slurry without other organic additives during gel casting, ANN model was presented for predicting the flexural strength and porosity of porous Si_3N_4 ceramics. Based on experimental results, a set of experimental data were used to develop the ANN model, and the results showed that the BP ANN approach gave quite encouraging predictions for the performances of porous Si_3N_4 ceramics, which indicated that BP ANN was a very useful and accurate tool for the prediction and optimization of porous Si_3N_4 ceramics performances. By means of the developed ANN model, the influencing factors of the performances of porous Si_3N_4 ceramics including monomer content, solid loading and the ratio of crosslinking agent to monomer, were investigated.

2. Experimental

2.1. Materials

Si_3N_4 powders (mean particle size: 0.37 μm, α phase >94 wt.%) employed in the experiment were commercially available materials. Al_2O_3 (mean particle size: 1.07 μm, 99% purity) and Y_2O_3 (mean particle size: 4.74 μm, 99.9% purity) were used as the sintering additives. For gel casting purpose, acrylamide (AM, $C_2H_3CONH_2$) and *N*,*N*′-methylenebisacrylamide (Merck, MBAM, $(C_2H_3CONH)_2(CH_2)$) were applied in the process of gel casting as monomers for polymerization. A dispersant (1 wt.%, ammonium salt of poly(acrylic acid)) was added to minimize agglomeration, and potassium persulphate (Merck, $K_2S_2O_8$) was used as initiator. A proper amount of polyacrylamide (PAM) with an average molecular weight approximately 3,000,000 may eliminate the surface exfoliation phenomenon of green body cast in air [16]. Ammonia aqueous was used as pH adjuster. All of these reagents are chemically pure.

2.2. Si_3N_4 ceramics preparation

In the first step, the PAM (2 wt.%, based on silicon nitride) and dispersant (1 wt.%, based on silicon nitride) were first completely dissolved in deionized water using mechanical stirring for 10 min, and then monomers were dissolved. The premix solution served as a dispersing media for the ceramic powders.

The next step is to add silicon nitride powders and suitable sintering additives (1 wt.%, Al_2O_3; 2 wt.%, Y_2O_3, based on silicon nitride) to the premix solution. The slurry, with different solid loading, was degassed for 20 min after rolling for 12 h in polyethylene bottles, using agate balls. The slurry was degassed for another 10 min when the initiator was added. All the above operations were conducted at room temperature. Afterwards, the slurry was cast into a nonporous cylindrical glass mold having the diameter of 40 mm and the height of 25 mm, which was then kept at 65 °C for 40 min. After the monomers had polymerized, the green bodies were demolded. After gel casting, the samples were dried in a commercial dryer at 20 °C with relative humidity of 98% for 140 h to avoid cracking and non-uniform shrinkage caused by rapid drying. The temperature of the binder removal was determined from the result of thermal gravimetric analysis (TGA). Thermogravimetric analysis showed that the temperature range of the binder removal was from 220 to 550 °C. Therefore, the samples containing organic binder were placed in a furnace and heated from 220 to 550 °C in air using a heating rate of 10 °C/h to control the gas release during pyrolysis of organic substances, and then temperature kept 550 °C for 8 h to burn out the residual organic substances thoroughly. After binder removal, sintering was performed at a heating rate of 10 °C/min and 1 h holding time at 1730 °C.

2.3. Characterization

The porosity of the sintered sample was measured by the Archimedes displacement method, using distilled water. The room temperature mechanical strength of the sintered bodies was determined by three-point flexural tests of specimens. The specimens were machined into test bars, Three-point bending strength was measured on bars using a span of 16 mm and a crosshead speed of 0.5 mm/min (Instron 1195; Instron, UK). By repeating the tests for silicon nitride three times for each specimen, all the results of Si_3N_4 ceramics in the paper are given as the mean values of three measurements.

Fracture surfaces of the sintered bodies were observed using scanning electron microscopy (SEM; S-570; Hitachi) to estimate the microstructure uniformity of the specimens without developing a huge grain growth. Pore-size distributions of the sintered body were measured using high-pressure porosimeter (Autoscan 33, Quantachrome Corp., USA).

3. ANN modeling of Si_3N_4 ceramics preparation

Artificial neural networks (ANN) are interconnected parallel systems consisting of simple processing elements (neurons), and use existing data to learn the functional relationships between inputs and outputs without prior assumption of the input–output relationship [13,17,18]. Therefore, ANNs have powerful advantages in practical application of complex systems.

Table 1
The design of orthogonal table $L_{16}(4^5)$.

Experiment no.	Solid loading (%)	Monomer content (%)	The ratio of crosslinking agent to monomer
1	30	10	0.50
2	30	15	0.33
3	30	20	0.25
4	30	25	0.20
5	40	10	0.33
6	40	15	0.25
7	40	20	0.20
8	40	25	0.50
9	50	10	0.25
10	50	15	0.20
11	50	20	0.50
12	50	25	0.33
13	60	10	0.20
14	60	15	0.50
15	60	20	0.33
16	60	25	0.25

The training of a neural network with appropriate data is a key requirement of a neural network approach. This means that the first step is to collect the training data sets which can be used to train the network. Among various influencing factors, solid loading ($\dot{m}_s$), monomer content ($\dot{m}_m$) and the ratio of crosslinking agent to monomer ($R_{c/m}$) are very critical in determining the performances of porous Si_3N_4 ceramics. Therefore, the influences of $\dot{m}_s$, $\dot{m}_m$ and $R_{c/m}$ on the performances of porous Si_3N_4 ceramics were investigated.

3.1. Orthogonal experimental design

Orthogonal experimental design is an effective mathematical method for multi-factor experimental design, and the collocation of the values of influencing factor is uniform and overall [15]. Orthogonal experimental results are also very effective to establish artificial neural networks (ANNs). In the paper, an orthogonal table $L_{16}(4^5)$ was used in the experiment, as shown in Table 1, and flexural strength and porosity of Si_3N_4 ceramics were set as investigation targets. Four levels were set for each influencing factor.

3.2. ANN modeling

In this study, a three-layer back propagation (BP) ANN architecture was adopted, and the structure of the ANN model for the prediction of the performances of porous Si_3N_4 ceramics is shown in Fig. 1. The first layer is the input layer with neurons representing input variables (e.g. solid loading, monomer content and the ratio of crosslinking agent to monomer). The last layer is the output layer with neurons representing the dependent variables (e.g. the flexural strength and porosity). Between them, there is a hidden layer containing neurons to help capture the non-linearity of the data. Both input layer and hidden layer have an additional bias neuron, respectively. Different layers are connected by weights (h_i). The ANN model is composed of three neurons in the input layer and two neurons

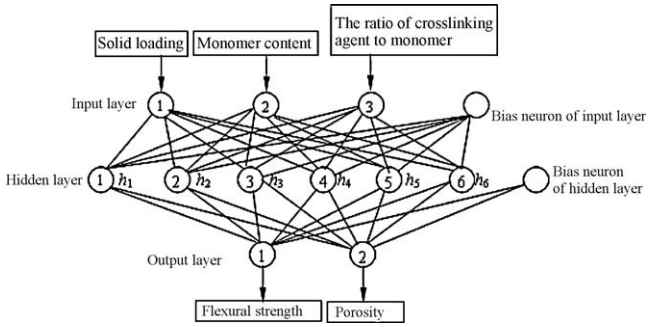

Fig. 1. Schematic view of the BP ANN for predicting performance of porous Si_3N_4 ceramics.

in the output layer. After several trials of different numbers of hidden neurons, six neurons were selected in the hidden layer. In Table 2, 16 data sets were used for the training of the ANN, and 5 data sets were used for the testing of the ANN model. The ANN is built by repeatedly adjusting weights (h_i) until the overall error between calculated and target outputs is approaching to the preset error criteria (10^{-4}). The detailed steps of the back-propagation (BP) algorithm performed in the network were reported elsewhere [19]. The established ANN model is delineated by the connection weights between the input and hidden layers and the connection weights between the hidden and output layers, which are listed in Tables 3 and 4, respectively. For the neural network, the momentum factor and learning rate are 0.95 and 0.35, respectively.

The orthogonal experimental results were used as the training data sets to develop ANN model. In order to validate the developed ANN model, the experimental data except the training data were required. Therefore, we carried out extra experiments to obtain data sets for testing the developed ANN model.

4. Results and discussion

4.1. Microstructural characteristics of the green body and the sintered body

The SEM photos of the green body and the sintered body are shown in Fig. 2. In Fig. 2(a), Si_3N_4 powders were homogeneously bound by organic binder. Pores in ceramic were formed during drying and organic binder removal from green body. At the same time, during sintering process, α-Si_3N_4 grains were converted into elongated β-Si_3N_4 grains, and then these fine elongated β-Si_3N_4 grains were jointed to form porous Si_3N_4 ceramics, as shown in Fig. 2(b). Fig. 3 shows the pore distribution of porous Si_3N_4 ceramics. The average pore size shown here is about 600.8 nm. The pores have an almost sharp distribution, and thus the pores size is uniform and less than 1 μm.

4.2. Predicting capability of the ANN model

Figs. 4 and 5 show the experimental values versus predicted values. As can be seen in Fig. 4, the ANN model is

Table 2
Experimental results of performance of porous Si_3N_4 ceramics.

	Experiment code							
	1	2	3	4	5	6	7	8
The training data sets for ANN model								
Flexural strength (MPa)	88.12 ± 0.78	87.80 ± 0.63	115.61 ± 0.61	153.1 ± 0.77	116.74 ± 0.68	160.92 ± 0.64	164.5 ± 0.82	134.88 ± 0.75
Porosity (%)	58.58 ± 0.02	59.72 ± 0.03	55.75 ± 0.02	57.65 ± 0.02	50.82 ± 0.01	53.54 ± 0.02	56.00 ± 0.03	61.59 ± 0.03
	Experiment code							
	9	10	11	12	13	14	15	16
The training data sets for ANN model								
Flexural strength (MPa)	182.42 ± 0.52	151.74 ± 0.77	62.06 ± 0.63	98.67 ± 0.70	134.3 ± 0.55	54.54 ± 0.69	55.54 ± 0.55	59.17 ± 0.71
Porosity(%)	51.19 ± 0.02	52.42 ± 0.01	61.92 ± 0.02	58.20 ± 0.02	49.52 ± 0.03	57.60 ± 0.02	54.66 ± 0.02	54.62 ± 0.01
	Experiment code							
	17	18	19	20	21			
The testing data sets for ANN model								
Flexural strength (MPa)	82.4 ± 0.02	135.72 ± 0.01	128.01 ± 0.02	160.08 ± 0.02	178.38 ± 0.01			
Porosity (%)	63.74 ± 0.02	57.38 ± 0.01	51.74 ± 0.02	53.20 ± 0.02	48.61 ± 0.01			

Table 3
Connection weights between the input layer and the hidden layer.

	h_1	h_2	h_3	h_4	h_5	h_6
Solid loading	−71.265	−8.6232	−1321.2	−3.869	146.41	−833.308
Monomer content	−171.449	−12.677	994.5	−4.145	201.538	−814.899
The ratio of crosslinking agent to monomer	−100.6404	−6.678	1952.5	−3.103	−83.584	−1671.311
Input bias	230.7505	10.2852	−905.2053	4.2492	−121.4657	1005.698

Table 4
Connection weights between the hidden layer and the output layer.

	h_1	h_2	h_3	h_4	h_5	h_6	Hidden bias
Flexural strength	−3.2199	−2.0505	−0.95638	−1.7745	1.4284	−4.9607	4.5292
Porosity	0.07168	−3.0295	1.0437	1.4248	1.6992	−0.90799	0.10451

very accurate in predicting the original training data sets. For a more convincing inspection of the accuracy of the ANN model, five data sets which are not included in the training data sets are tested (see Fig. 5). It indicates that predicted values correspond with experimental values for the flexural strength and porosity. Therefore, the ANN model can give much better prediction, and the performance of the model is quite satisfactory.

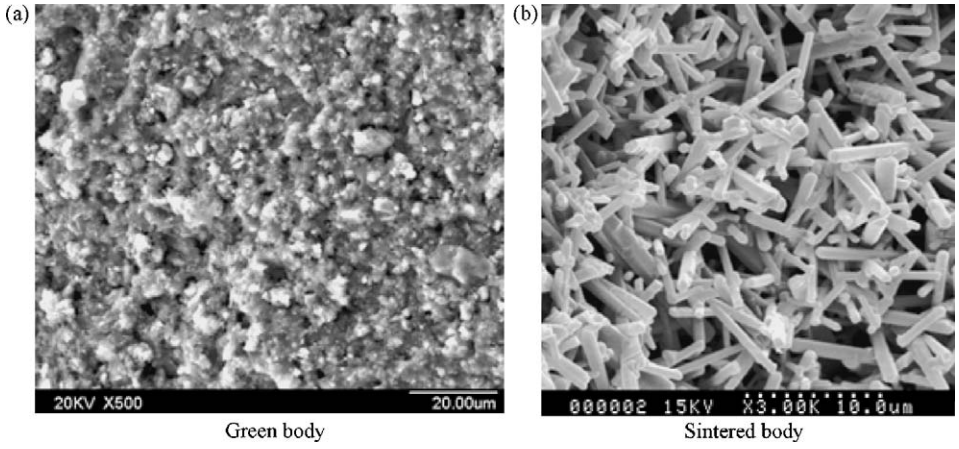

Fig. 2. SEM fracture surface of samples.

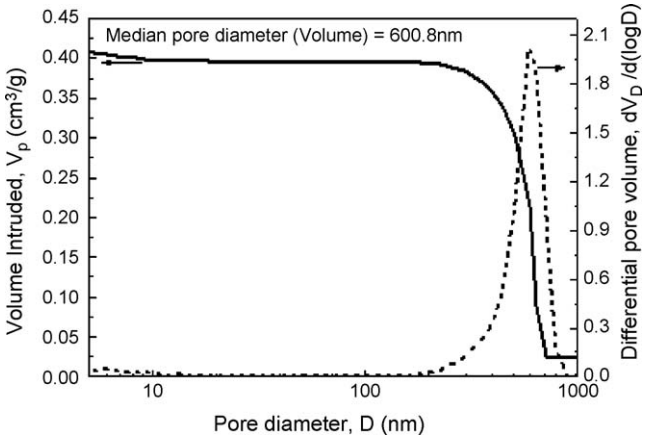

Fig. 3. Pore distribution of porous Si_3N_4 ceramics.

4.3. The influences of solid loading and monomer content on performances of porous Si_3N_4 ceramics

By using the developed ANN model simulation, the influences of solid loading and monomer content on the flexural strength and porosity of porous Si_3N_4 ceramics were investigated, and the predicted results are shown in Figs. 6 and 7.

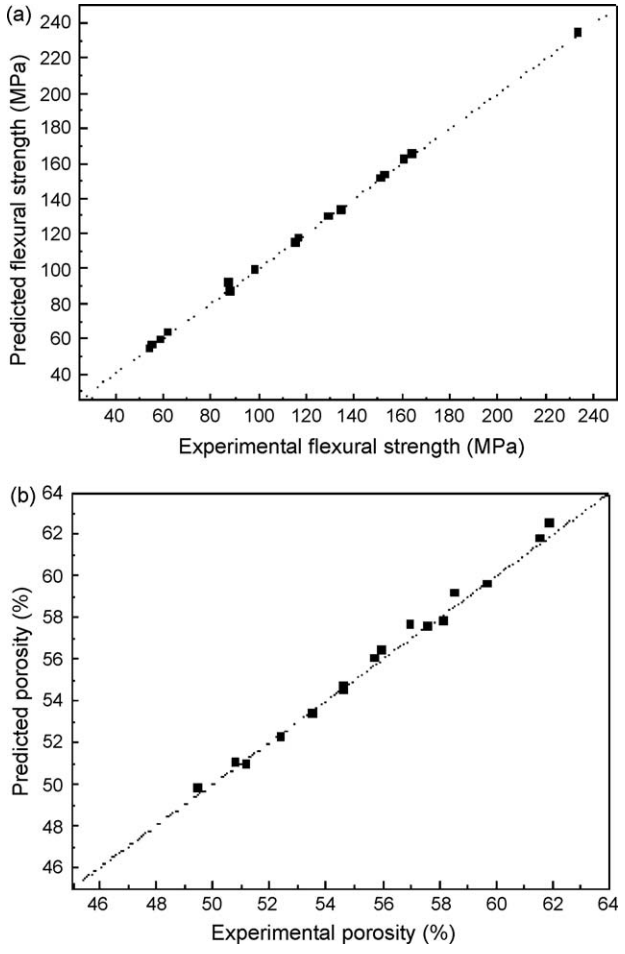

Fig. 4. Experimental vs. predicted values of flexural strength and porosity of porous Si_3N_4 ceramics for training of the ANN model.

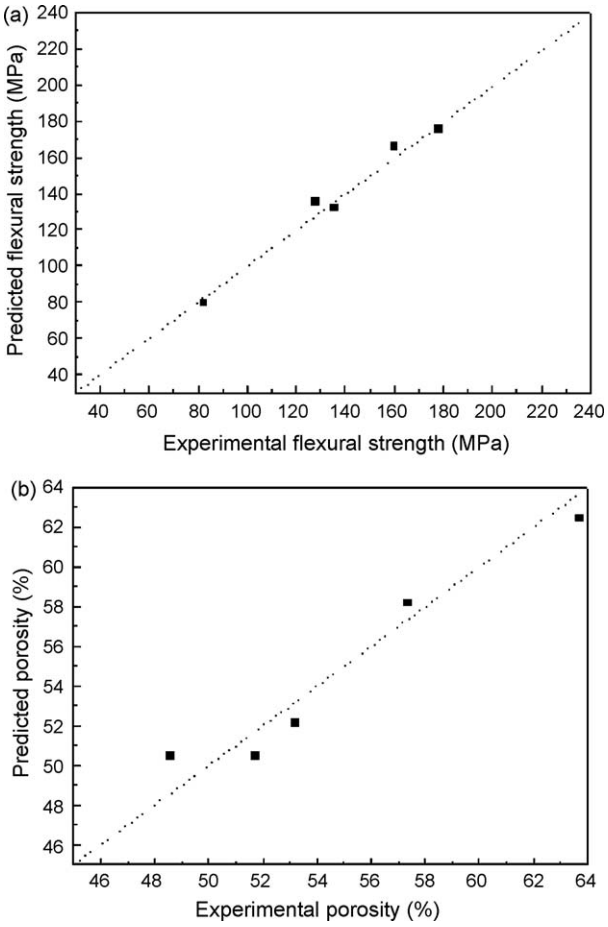

Fig. 5. Experimental vs. predicted values of flexural strength and porosity of porous Si_3N_4 ceramics for testing of the ANN model.

At a given monomer content, with increasing solid loading, the flexural strength first increases and then decreases, and the porosity of sintering body monotonically decreases (see Figs. 6 and 7).

In Fig. 6, the variation trend of flexural strength of sintering body with solid loading are similar at different monomer contents, and there is an optimum solid loading at a given monomer content. Solid loading has complex influences on the flexural strength of porous Si_3N_4 ceramics, and the reasons are as follows: Solid loading has a great influence on the rheological properties of Si_3N_4 slurry. The spaces between Si_3N_4 particles in slurry are affected by the solid loading, according to the Woodcocl equation [20]:

$$\frac{h}{d} = \left(\frac{1}{3\pi\phi} + \frac{5}{6}\right)^{1/2} - 1 \quad (1)$$

where h is the space between Si_3N_4 particles in a slurry; d is the diameter of Si_3N_4 particles; ϕ is the solid loading. It is known from Eq. (1) that increasing the solid loading makes the space between Si_3N_4 particles in slurry decrease, and this leads to an increase of the viscosity of the slurry. The viscosity of slurry influences molding properties (such as uniformity of slurry, inner stresses distribution and the probability of occurrence of

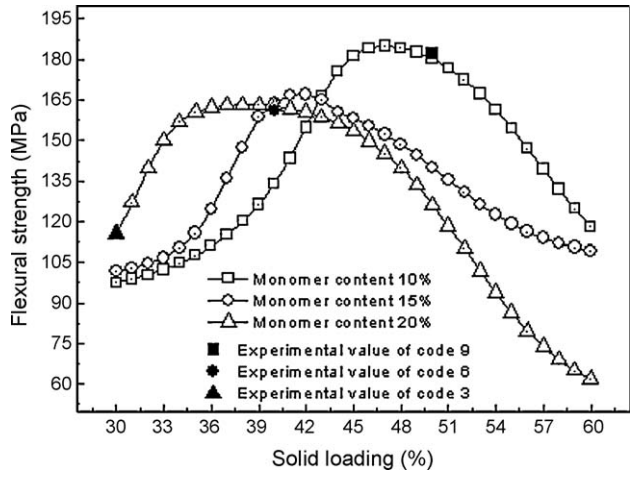

Fig. 6. The prediction of the influences of solid loading and monomer content on flexural strength at the ratio of crosslinking agent to monomer 0.25.

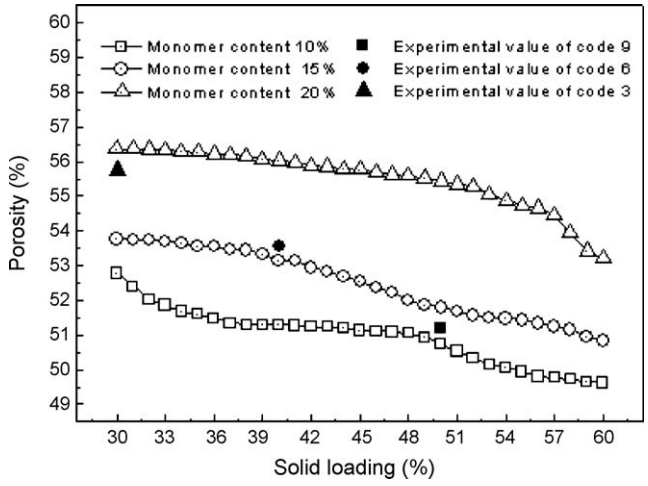

Fig. 7. The prediction of the influences of solid loading and monomer content on porosity at the ratio of crosslinking agent to monomer 0.25.

micro-cracks in ceramics), and finally it influences the flexural strength of Si_3N_4 sintered body. Solid loading has a great influence on the shrinkage during drying and sintering. Increasing the solid loading makes drying and sintering shrinkage decrease due to the space between Si_3N_4 particles, which makes inner stresses and micro-cracks of a porous Si_3N_4 sintered body decrease, and finally the flexural strength of Si_3N_4 sintered body increase. Solid loading also affects the density of the sintered body. The density of Si_3N_4 sintered body increase with solid loading, which makes the sintering interfaces of Si_3N_4 particles increase, and thus the flexural strength of Si_3N_4 sintered body increase.

According to above discussions, when solid loading is too low, the space between Si_3N_4 particles in slurry is large, and this results in the increase of drying and sintering shrinkages and the increase of the probability of occurrence of micro-cracks in a green body. In the meantime, too low solid loading makes the decrease of the density and the sintering interfaces of Si_3N_4 particles in a sintered body. Therefore, the flexural strength of porous Si_3N_4 sintered body is low at too low solid loading, and increasing solid loading may make the flexural strength increases. However, when solid loading is too high, the non-uniformity of slurry results in the increase of probability of occurrence of micro-cracks in a green body, and finally this results in the decrease of the flexural strength. Therefore, for flexural strength of sintering body at given monomer content, there is an optimum solid loading (see Fig. 6). At the optimum solid loading, the uniformity of slurry is well, the drying shrinkage and warpage are small. Thus high performance of green body results in the highest flexural strength of sintering body at the optimum solid loading.

With the increase of monomer content, the optimum solid loading decreases, and the corresponding maximum flexural strength decreases too (see Fig. 6). When monomer content is low, the crosslink density of gel is low, and the stability and uniformity of green body is poor. In this case, increasing solid loading makes the space between Si_3N_4 particles in slurry decrease, the uniform slurry can be achieved at high solid loading, and thus the optimum solid loading is high at low monomer content. However, when monomer content is high, the crosslink density of gel is great, and the stability and the uniformity of slurry are well. In this case, when solid loading is high, the viscosity of the slurry increases, and the high viscosity of slurry reduces molding properties. Thus, when monomer content is high, the optimum solid loading is low (see Fig. 6).

In Fig. 7, the porosity of sintering body monotonically decreases with the increase of solid loading at a given monomer content. Increasing solid loading makes the density of sintering body increases, which results in the decrease of porosity.

Fig. 7 also shows that the porosity of sintering body increases with the increase of monomer content. In the experiment, the porous ceramics is prepared by only increasing monomer content in the slurry without other organic additives during gel casting. Here, monomer and crosslinking agent not only can form macromolecular network to hold the ceramic particles together, but also can play the leading role in the formation of pores during the preparation of porous Si_3N_4 ceramics. Before green body of ceramics can be sintered, the organic processing aids (mainly monomer) that are incorporated in the green body during gel casting must be removed. The pores of sintered body mainly originate from the residual micro-space of the organic processing aids in the green body during organic binder burnout. Therefore, with the increase of monomer content, the porosity of sintered body increases.

4.4. The influences of the ratio of crosslinking agent to monomer on performances of porous Si_3N_4 ceramics

By using the developed ANN model simulation, the influences of the ratio of crosslinking agent to monomer on porosity and flexural strength of porous Si_3N_4 ceramics were investigated at solid loading 40%, and the predicted results are shown in Figs. 8 and 9. The predicted results show that the porosity increases and the flexural strength of sintered body decreases with the increase of the ratio of crosslinking agent to monomer.

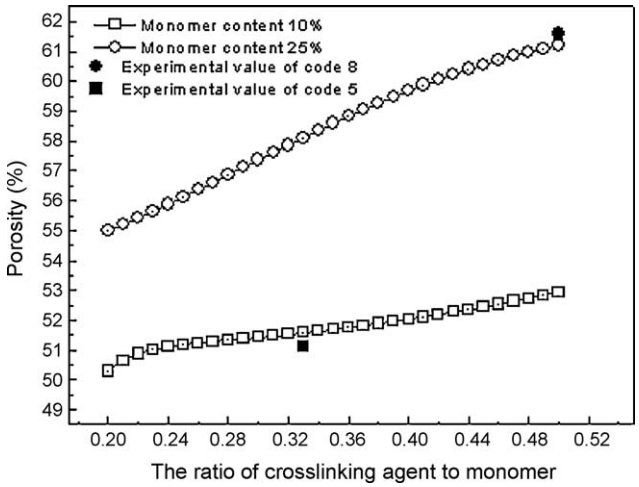

Fig. 8. The prediction of the influences of the ratio of crosslinking agent to monomer on porosity.

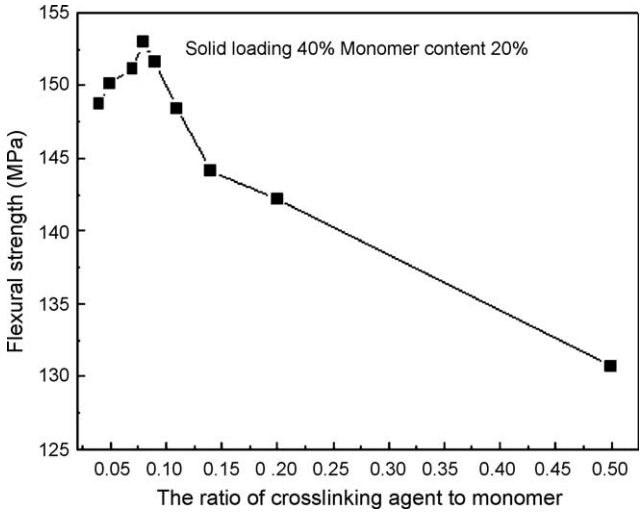

Fig. 10. The experimental results of the influences of the ratio of crosslinking agent to monomer on the flexural strength of sintered body.

Since the increase of crosslinking agent makes the crosslink density of cross-linked polymer gels in green body increase, the distribution of ceramics particles is more uniform, the drying shrinkage is smaller, and thus the porosity of sintering body increases (see Fig. 8).

The kernel of the gel casting process is the monomers solution that polymerizes to form a gel. As a rule, with the increase of the ratio of crosslinking agent to monomer, crosslinking points of gel become more, which makes the three-dimensional network structures of cross-linked polymer gels compact, and then the ceramic particle distribution in the network of gel is more uniform. Consequently, the probability of micro-crack occurrence decrease during the drying of the green body, and finally the flexural strength of sintering body increases. However, when the ratio of crosslinking agent to monomer is too high, the three-dimensional network structures of cross-linked polymer gels are coarse so as to make the probability of micro-crack occurrence increase during the drying of the green body, and then the flexural strength of sintering body decreases [21]. In Fig. 9, due to too high ratio of crosslinking agent to monomer, the flexural strength decreases with the increase of the ratio of crosslinking agent to monomer.

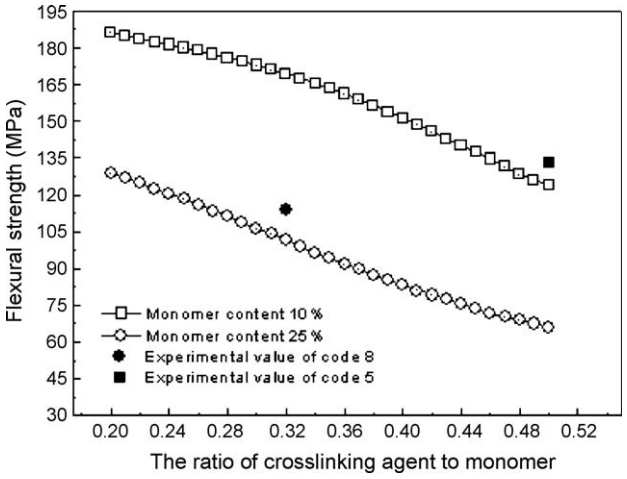

Fig. 9. The prediction of the influences of the ratio of crosslinking agent to monomer on flexural strength at solid loading 40%.

In the meantime, when the cross-linker content is too low, the three-dimensional network structure of cross-linked polymer gels is loose, which results in the non-uniform distribution of Si_3N_4 powders in green body, and finally the flexural strength of sintering body also decreases. In order to further investigate the influence of the ratio of crosslinking agent to monomer on the flexural strength of porous Si_3N_4 ceramics, the experiment was conducted when the ratio varied from 0.04 to 0.5 (solid loading and monomer content are 40% and 20%, respectively), and the experimental results are shown in Fig. 10.

Fig. 10 shows that the ratio of crosslinking agent to monomer has an optimum value, where the flexural strength of green body reaches maximum value. When the ratio of crosslinking agent to monomer varies from 0.2 to 0.5, the experiment results in Fig. 10 show that the flexural strength decreases with the increase of the ratio of crosslinking agent to monomer, which is consistent with predicted results in Fig. 9. Therefore, the developed ANN model can give much better predictions for the performances of porous Si_3N_4 ceramics.

5. Conclusions

In this study, based on orthogonal experimental results of porous Si_3N_4 ceramics by gel casting preparation, a three-layer BP ANN model was developed for the prediction and optimization of porous Si_3N_4 ceramics performances. The results showed that the BP ANN approach gave quite encouraging predictions for the performances of porous Si_3N_4 ceramics, which indicated that BP ANN was a very useful and accurate tool for performances analysis of porous Si_3N_4 ceramics.

By using the developed ANN model, the influences of the compositions on performances of porous Si_3N_4 ceramics were investigated, and some important conclusions were drawn as

follows: (1) there is an optimum solid loading where the flexural strength can achieve a maximum value, and the optimum solid loading decreases with the increase of monomer content; (2) the porosity of sintering body monotonically decreases with the increase of solid loading, and it increases with monomer content; (3) the ratio of crosslinking agent to monomer has an optimum value where the flexural strength of sintering body is highest; (4) the porosity of sintering body monotonically increases with the increase of the ratio of crosslinking agent to monomer.

Acknowledgments

This work was supported by the National Natural Science Foundation of China (90816018), New Century Excellent Talents in University (NECT-05-0838) and Xi'an Science and Technology Program (CXY08006(1)).

References

[1] O. Lyckfeldt, J.M.F. Ferreira, Processing of porous ceramics by 'starch consolidation', J. Eur. Ceram. Soc. 18 (2) (1998) 131–140.
[2] C. Kawai, T. Matsuura, A. Yamakawa, Separation–permeation performance of porous Si_3N_4 ceramics composed of columnar β-Si_3N_4 grains as membrane filters for microfiltration, J. Mater. Sci. 34 (5) (1999) 893–896.
[3] J.F. Yang, T. Ohji, S. Kanzaki, A. Díaz, S. Hampshire, Microstructure and mechanical properties of silicon nitride ceramics with controlled porosity, J. Am. Ceram. Soc. 85 (6) (2002) 1512–1516.
[4] C. Kawai, A. Yamakawa, Effect of porosity and microstructure on the strength of Si_3N_4: designed microstructure for high strength, high thermal shock resistance, and facile machining, J. Am. Ceram. Soc. 80 (10) (2002) 2705–2708.
[5] P. Sepulveda, J.G.P. Binner, Processing of cellular ceramics by foaming and in situ polymerisation of organic monomers, J. Eur. Ceram. Soc. 19 (12) (1999) 2059–2066.
[6] O.O. Omatete, M.A. Janney, R.A. Strehlow, Gelcasting—a new ceramic forming process, Am. Ceram. Soc. Bull. 74 (10) (1991) 1641–1649.
[7] M.A. Janney, O.O. Omatete, C.A. Walls, Development of low-toxicity gelcasting systems, J. Am. Ceram. Soc. 81 (3) (1998) 581–591.
[8] Y.L. Wang, J.J. Hao, Z.M. Guo, Study on the influencing factors of green strength by gel casting, J. Mater. Sci. Eng. 25 (2) (2007) 262–264.
[9] Y.F. Gu, X.Q. Liu, G.Y. Meng, D.K. Peng, Porous YSZ ceramics by water-based gelcasting, Ceram. Int. 27 (1) (1999) 1–7.
[10] Y.F. Liu, X.Q. Liu, G.Y. Meng, Porous mullite ceramics from national clay produced by gelcasting, Ceram. Int. 25 (8) (2001) 705–709.
[11] D.J.A. Netz, P. Sepulveda, V.C. Pandolfelli, A.C.C. Spadaro, Potential use of gelcasting hydroxyapatite porous ceramic as an implantable drug delivery system, Int. J. Pharm. 213 (1–2) (2001) 117–125.
[12] F.S. Ortega, F.A.O. Valenzuela, C.H. Scuracchio, V.C. Pandolfelli, Alternative gelling agents for the gelcasting of ceramic foams, J. Eur. Ceram. Soc. 23 (1) (2003) 75–80.
[13] P.A. Lucon, R.P. Donovan, An artificial neural network approach to multiphase continua constitutive modeling, Compos. B: Eng. 38 (7–8) (2007) 817–823.
[14] A.M. Remennikov, T.A. Rose, Predicting the effectiveness of blast wall barriers using neural networks, Int. J. Impact. Eng. 34 (12) (2007) 1907–1923.
[15] D.Y. Fan, Y.H. Chen, Probability Theory and Mathematical Statistics, Zhejiang University Press, China, 1996, pp. 215–220.
[16] J.T. Ma, Z.P. Xie, H.Z. Miao, Gelcasting of alumina ceramics in the mixed acrylamide and polyacrylamide systems, J. Eur. Ceram. Soc. 23 (13) (2003) 2273–2279.
[17] I. Fikret, Artificial neural network predictions of polycyclic aromatic hydrocarbon formation in premixed *n*-heptane flames, Fuel Process. Technol. 87 (11) (2006) 1031–1036.
[18] S. Mucahit, A. Sedat, ANN model for prediction of powder packing, J. Eur. Ceram. Soc. 27 (2–3) (2007) 641–644.
[19] D. Guo, Y.L. Wang, J.T. Xia, C. Nan, L.T. Li, Investigation of $BaTiO_3$ formulation: an artificial neural network (ANN) method, J. Eur. Ceram. Soc. 22 (11) (2002) 1867–1872.
[20] H.A. Barnes, J.F. Hutton, K. Walers, An Introduction to Rheology, Elsevier Press, Oxford, 1989.
[21] H.J. Wang, S.H. Jia, Y.L. Wang, Z.H. Jin, Gelcasting process of silicon nitride ceramics, J. Xi'an Jiaotong Univ. China 35 (4) (2001) 403–406.